ADVANCES IN ATMOSPHERIC SCIENCES, VOL. 25, NO. 4, 2008, 597–609

Revisiting Effect of Ocean Diapycnal Mixing on Atlantic Meridional Overturning Circulation Recovery in a Freshwater Perturbation Simulation

YU Lei[1,3] (于 雷), GAO Yongqi[1,2] (郜永祺), WANG Huijun[*1] (王会军), and Helge DRANGE[1,2]

[1] *Nansen-Zhu International Research Center, Institute of Atmospheric Physics, Chinese Academy of Sciences, Beijing* 100029

[2] *Nansen Environmental and Remote Sensing Center/Bjerknes Centre for Climate Research, Bergen, Norway*

[3] *Graduate University of Chinese Academy of Sciences, Beijing* 100049

(Received 10 May 2007; revised 18 December 2007)

ABSTRACT

The effects of ocean density vertical stratification and related ocean mixing on the transient response of the Atlantic meridional overturning circulation (AMOC) are examined in a freshwater perturbation simulation using the Bergen Climate Model (BCM). The results presented here are based on the model outputs of a previous freshwater experiment: a 300-year control integration (CTRL), a freshwater integration (FW1) which started after 100 years of running the CTRL with an artificially and continuously threefold increase in the freshwater flux to the Greenland-Iceland-Norwegian (GIN) Seas and the Arctic Ocean throughout the following 150-year simulation. In FW1, the transient response of the AMOC exhibits an initial decreasing of about 6 Sv (1 Sv=10^6 m^3 s^{-1}) over the first 50-year integration and followed a gradual recovery during the last 100-year integration. Our results show that the vertical density stratification as the crucial property of the interior ocean plays an important role for the transient responses of AMOC by regulating the convective and diapycnal mixings under the enhanced freshwater input to northern high latitudes in BCM in which the ocean diapycnal mixing is stratification-dependent. The possible mechanism is also investigated in this paper.

Key words: North Atlantic meridional overturning circulation, enhanced freshwater forcing, diapycnal mixing

DOI: 10.1007/s00376-008-0597-0

1. Introduction

The Atlantic meridional overturning circulation (AMOC) is an active component of the global climate system (Rahmstorf and Ganopolski, 1999). AMOC is a vertical circulation loop and can be conceptually represented by four main branches. The first branch is the warm and saline water flowing northward with the North Atlantic Current (NAC) at the surface or near surface. The second branch involves the descending dense waters formed by the convective mixing in the high northern latitudes, known as the North Atlantic Deep Water (NADW) and the third branch in North Atlantic (NA) comprises mainly the southward-flowing of the NADW with the deep western boundary currents (DWBC; Gao et al., 2003; Bentsen et al., 2004). Finally, in the low latitudes and in the Southern Ocean, the loop is closed by upwelling of deep water through the pycnocline as the fourth branch. The upward motion is generally considered to be more widely distributed over all ocean basins (Stommel and Araons, 1960), although it has been shown that the upwelling may be particularly strong close to the ocean margins and to rough topography (Moum et al., 2002; Garabato et al., 2004).

Early studies suggested that two main different vertical mixing processes, convective and diapycnal mixing, play important roles in regulating the transient

*Corresponding author: WANG Huijun, wanghj@mail.iap.ac.cn

changes of AMOC (e.g., Nilsson and Walin, 2001; Gao et al., 2003; Bentsen et al., 2004). Unstable stratification in upper ocean layers caused by buoyancy loss at the surface (i.e., the cooling or the evaporation of sea surface) may lead to convective mixing of water mass, which transports the dense water downward into the interior isopycnic layers below the mixed layer (ML) and absorbs the new water masses into the ML water. Different from convective mixing in upper ocean layers, the diapycnal mixing occurs among the isopycnic layers in intermediate and deep ocean within mid- and low-latitudes (Marotzke and Scott, 1999), is mainly caused by the breaking of internal waves (Garrett and Laurent, 2002; Wunsch and Ferrari, 2004) and leads to the downward mixing of heat which is balanced by a broad upwelling motion in steady state, connecting the northward flow of light surface waters. Although the diapycnal mixing is parameterized by a constant in space or time in most OGCM, it is in fact strongly influenced by stratification (reversely proportional to the density stratification) (Gargett, 1984). The impacts of the two mixing motions associated with ocean stratification on the AMOC have been the foci of a series of observational and numerical studies. Isachsen et al. (2007) pointed out that NADW as the sinking branch of AMOC is mainly formed by winter convective mixing in the GIN Seas, the Irminger and Labrador seas, while Gao et al. (2003) suggests that the NA overflow waters (OW) from the GIN Seas, the penetration of the western boundary currents, the ventilation of the subtropical surface waters, the vertical density stratification and the meridional overturning are all critically dependent on the applied strength of the isopycnal and diapycnal mixing.

Initiated with the paleo record and recent observations (e.g., Peterson et al., 2002; Dickson et al., 2002), numerical studies have been widely performed to investigate the impact of the NA fresh water perturbation in the high latitudes on the AMOC. Most studies suggest the weakening or shutting down of AMOC if there is a net flux of freshwater added to the high northern latitudes (Manabe and Stouffer, 1997; Schiller et al., 1997; Vellinga et al., 2002; Zhang et al., 2004), but the recovery of AMOC have also been reported (Munk and Wunsch, 1998; Otterå et al, 2004) and even the strengthened AMOC is found in some theoretical OGCMs (e.g., Nilsson and Walin, 2001; Mohanmmad and Nilsson, 2004). It is suggested that the parameterization of the vertical mixing in the OGCMs is one of the key issues to cause the different responses of the AMOC to the enhanced fresh water forcing. Some studies suggested that the North Atlantic freshening results in a decrease in sea surface salinity (SSS) and surface potential density (SPD), stabilizing upper ocean layers, reducing NADW formation, and, in turn, leading to a weakening or collapse of AMOC (e.g., Rahmstorf, 1996; Manabe and Stouffer, 1997; Tziperman, 2000). On the other hand, a number of studies emphasize the potential importance of the diapycnal mixing: the decreased stratification due to the reduced formation of NADW may increase the diapycnal mixing on the broad low latitudes and the southern ocean, which triggers the upwelling that transports the deep dense water mass upward, resulting in the recovery of AMOC (e.g., Munk and Wunsch, 1998; Huang, 1999; Oliver et al., 2005). Behind these views there is an implication in the role of the ocean vertical stratification: all these responses to the freshwater forcing are linked to the changes of vertical stratification.

In a recent study, Otterå et al. (2004) found that the AMOC showed an initial reduction followed by a recovery in a 150-yr integration using BCM with continuous enhanced fresh water forcing in the high northern latitudes. In the present study, using the model output from Otterå et al. (2004), we will focus on the transient changes in ocean convective and diapycnal mixing processes parameterized as density stratification dependent in BCM and explore their roles in modulating the transient change of the AMOC.

The paper is organized as follows: The model description and the set-up of the freshwater experiment are described in section 2. The results are presented in section 3. The possible feedback and mechanism are discussed in section 4 and conclusions are given in section 5.

2. Model description and freshwater experiment design

2.1 *Model description*

The atmosphere component of BCM is the spectral general circulation model ARPEGE/IFS from Météo-France (Déqué et al., 1994). In the present study, ARPEGE/IFS is run with a truncation at wave number 63 (TL63), and a time-step of 1800 s. The grid point calculations are carried out with a grid of horizontal resolution of about 2.8°. A total of 31 vertical levels are employed, which range from the surface to 0.01 hPa (20 layers in the troposphere). Several explicit physical parameterizations are applied for diagnosing or calculating the flux of mass, energy and/or momentum due to a specific physics process. Further details of the ARPEGE model are provided in Furevik et al. (2003).

The oceanic component of the BCM is the Miami Isopycnic Coordinate Ocean Model (MICOM, Bleck et al., 1992). The horizontal grid has a 2.4° resolution along the equator with one pole over Siberia and the

other is the South Pole. There are 24 layers in the vertical, of which the uppermost ML has a spatial and temporal varying density and 23 isopycnal layers below ML with prescribed potential density ranging from 1024.12 to 1028.10 g m^{-3}. Convective adjustment is included to remove the unstable water column.

In MICOM, the diapycnal mixing is parameterized as stratification-dependent. The diapycnal mixing coefficient, K_d follows Gargett's (1984) expression:

$$K_d = 3 \times 10^{-7} \times \frac{1}{N} \quad (1)$$

where,

$$N = \sqrt{\frac{g}{\rho}\frac{\partial \rho}{\partial z}},$$

N is the Brunt-Vaisala frequency (units: s^{-1}), ρ is the density of ocean water (units: kg m^{-3}) and g is the acceleration of gravity (units: m s^{-2}). The numerical implementation of the diapycnal mixing follows the scheme of McDougall and Dewar (1998).

The OASIS (ocean atmosphere sea ice soil) coupler has been used to couple the atmosphere and ocean models. The main purposes of OASIS are to synchronize the models, so the faster running model can wait for the other model until they are both integrated over a prescribed time interval (24 h in this study), to read the exchanged fields from the source model, to apply weight coefficients for the interpolations, and finally, to write the new fields to the target model.

In the BCM simulation, SSS and SST are flux adjusted based on annual repeated heat and freshwater fluxes diagnosed as weekly averaged fields from the spin-up integration of the coupled system.

2.2 *Freshwater experiment design*

A general description of the set-up of the freshwater experiment has been given in Otterå et al. (2004), and only a brief outline is given here. The basis for the freshwater experiment (FW1) is the modern state as simulated by the 300-yr control (CTRL) run with the BCM (Furevik et al., 2003). The FW1 is carried out by perturbing the modeled state in year 100 of CTRL with a threefold increase in the river runoff to the high northern latitude seas, and thereafter the model is run for another 150 years. The anomalous freshwater input is continuously and instantaneously added to the coastal regions in the GIN Seas and the Arctic Ocean during the 150-yr integration. For the detailed spatial distribution of the fresh water perturbation, please refer to Fig. 1 in Otterå et al. (2004)

In CTRL, the river runoff is about 0.1 Sv, comparable to the estimate by Aagaard and Carmack (1989) for the present-day climate system. In FW1, the river runoff is increased to 0.4 Sv, similar to the simulated increase in the total freshwater input obtained by a quadrupling of the pre-industrial CO_2 level (Manabe and Stouffer, 1994). The 0.4 Sv freshwater perturbation is also believed to be consistent with the melt water entering the high northern oceans during the last deglaciation (Simonsen, 1996).

3. Results

3.1 *The response of AMOC and net northward transports of heat and salt*

The maximum rate of the AMOC, essentially representing the total northward/southward water mass transport, is often used as an indicator to the strength of the AMOC. Figure 1 shows the time series of the simulated AMOC (strength between 20°–50°N) in FW1 and CTRL. It should be mentioned that the time series in all plots except Fig. 14 in this paper have been smoothed using a 5-year running mean filter. In CTRL, the AMOC exhibits decadal variations around the mean value of about 18 Sv. This value is close to the results from other numerical studies (e.g., Zhou et al., 2005). In FW1, the major change in the AMOC takes place over the first 50 years, with suppressed decadal variability and a drop in the strength of up to about 6 Sv. There is a gradual and constant recovery of the AMOC over the following 100-year integration, reaching a value of about 17 Sv in year 150. There is a drift in the simulated AMOC in CTRL with the linear trend of 1.8 Sv $(100\ yr)^{-1}$. However, the linear trend in the simulated AMOC in FW1 is 3.0 Sv $(100\ yr)^{-1}$. Therefore, it is fair to conclude that there is a recovery of the AMOC in FW1.

With the weakening and recovery of AMOC, the northward transport of heat and salt into the NA subpolar region follow a similar pattern as indicated in Fig. 2. During the first 50 years, the salt transport

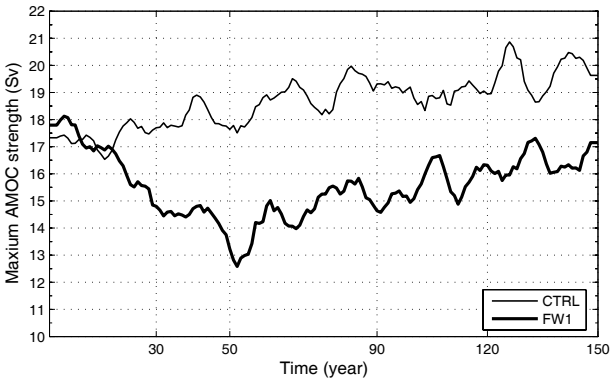

Fig. 1. Time series of the simulated AMOC (Sv) in FW1 (bold curve) and CTRL (thin curve).

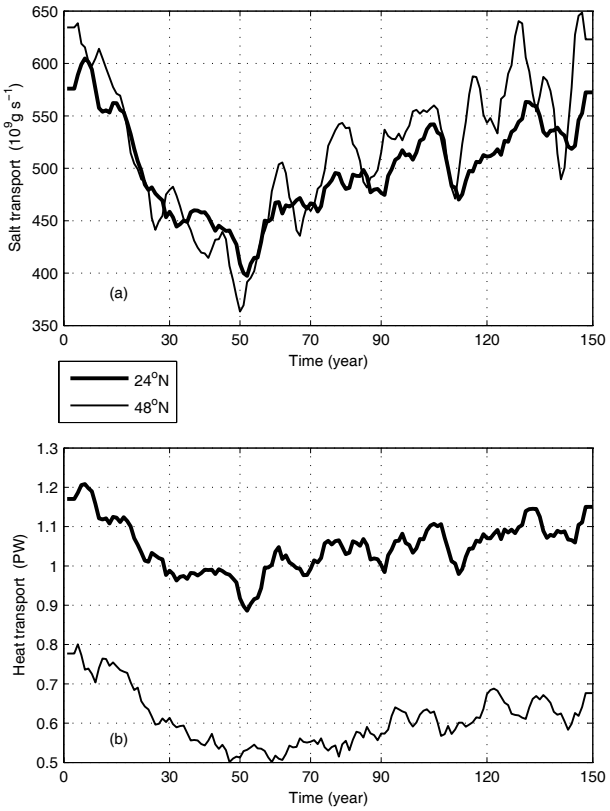

Fig. 2. The time series of (a) northward salt and (b) heat transport in FW1 across sections of 24°N (bold black curve) and 48°N (thin black curve) in NA.

decreases quickly by about 250×10^9 g s^{-1} and 300×10^9 g s^{-1} at 24°N and 48°N respectively, and gradually recovers to the values at the initial level. For heat transport, during the first 50-year integration, it drops down from about 1.2 PW to 0.9 PW at 24°N and from around 0.8 PW to about 0.5 PW at 48°N and recovers gradually to the values at the initial level, too.

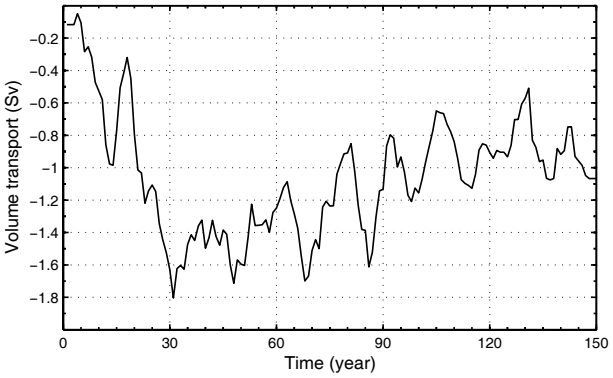

Fig. 3. The time series of the anomaly (FW1-CTRL) of the total southward-flowing dense water transport (water mass with potential densities greater than 27.63) across GSR.

The time series of the anomaly (FW1−CTRL) of total southward-flowing dense water transport across the Greenland-Scotland Ridge (GSR) (Fig. 3) shows that dense water transport drops down more quickly than the northward heat and salt transport in the mid-latitudes, implying the quick response of the dense water in the GIN Seas.

3.2 *The response of sea surface*

Figure 4 shows the anomalies (FW1−CTRL) in SSS, SST and SPD during the first 30 years of integration. In the sub-polar region, the maximum freshening is about 0.5 psu (1 psu$\approx 10^{-3}$) mainly found in the Labrador Sea (Fig. 4a). The freshening of seawater results in the decreased SPD in the sub-polar region (45°–65°N, Fig. 4c).

However, although the enhanced freshwater input is maintained during the whole 150-year integration, the SSS and SPD in the sub-polar gyre still start to

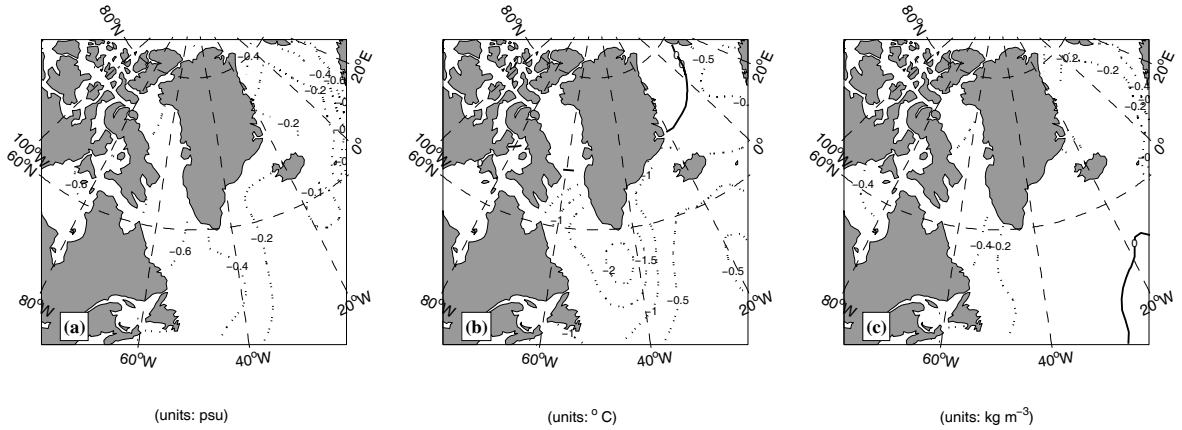

Fig. 4. The anomalies (FW1−CTRL) of the (a) SSS, (b) SST, and (c) SPD in the sub-polar region during the first 30-yr integration.

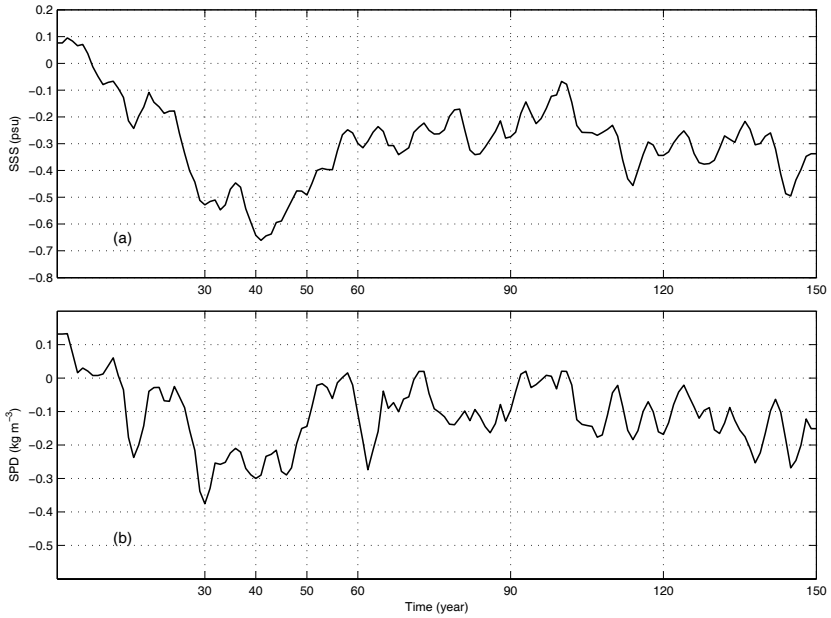

Fig. 5. The time series of the anomalies (FW1−CTRL) of the regional averaged (a) SSS and (b) SPD in the sub-polar region.

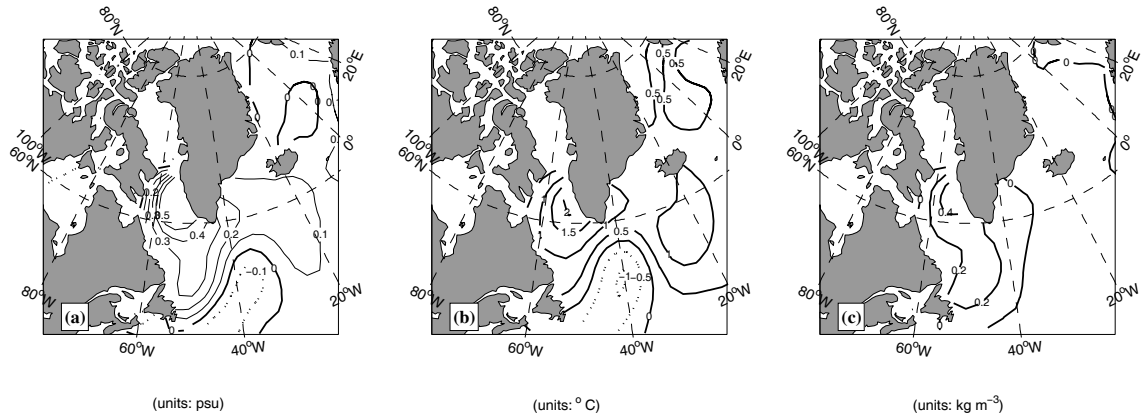

Fig. 6. The differences in the (a) SSS, (b) SST, and (c) SPD between the mean during the last 60-yr integration and that during the first 30-yr integration in FW1.

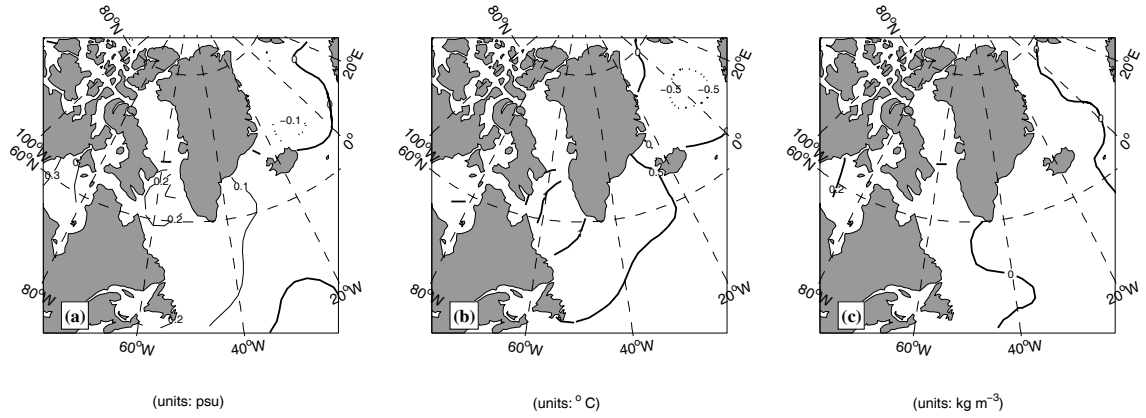

Fig. 7. Same as Fig. 6 but for CTRL.

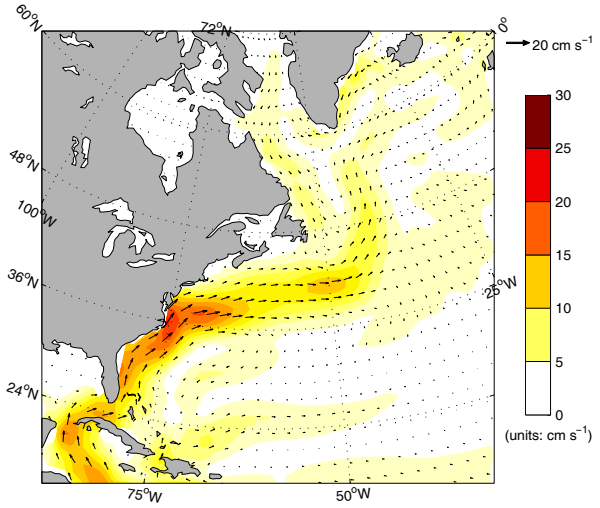

Fig. 8. The mean surface currents (arrows) and the difference in the surface ocean currents between the last 60-yr integration and the first 30-yr integration (in color) in FW1.

recover after about 40 years as shown in Fig. 5. It follows that the regional averaged SSS rapidly decreases during the first 40 years, and then recovers gradually (Fig. 5a), and that the variation of SPD is highly associated with that of SSS (Fig. 5b).

To examine the drift in sea surface features in CTRL and the time evolution of sea surface features in FW1, Figs. 6 and 7 show the difference of the SSS, SST and SPD between the mean of the last 60-yr integration and that of the first 30-yr integration in FW1 and CTRL respectively. An increase in SSS and SST with the magnitudes of 0.4 psu and 1.5°C in the Labrador and GIN Seas can be found in FW1, whereas an increase in SPD can only be found in the Labrador Sea (Fig. 6). In CTRL, the increase in SSS and SST is confined to the northern NA (GIN Seas are not the case) and the increase in SPD takes place in the Labrador Sea (Fig. 7). However, the increase in CTRL is weaker than that in FW1, implying that the increase in SSS, SST and SPD in FW1 can not be fully explained by

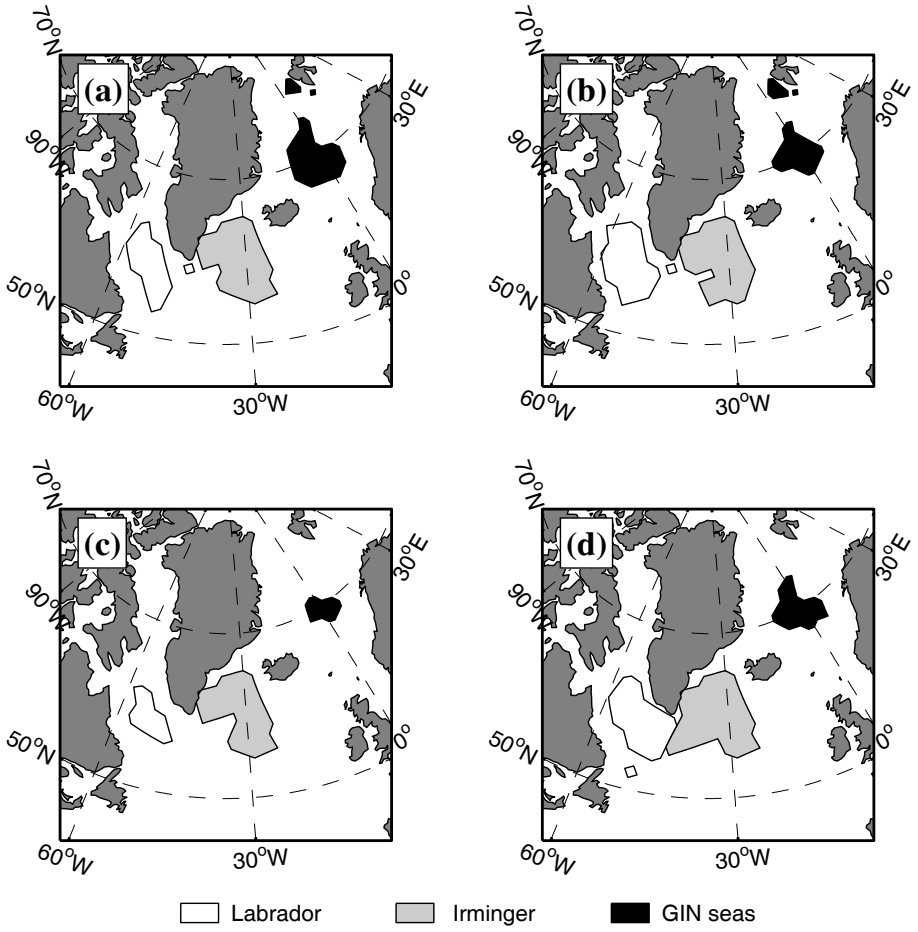

Fig. 9. The area where the deep convection takes place in winter. (a) and (b) show the results during the first 40-yr and the last 60-yr integration in CTRL respectively. (c) and (d) are the same as (a) and (b) but for FW1.

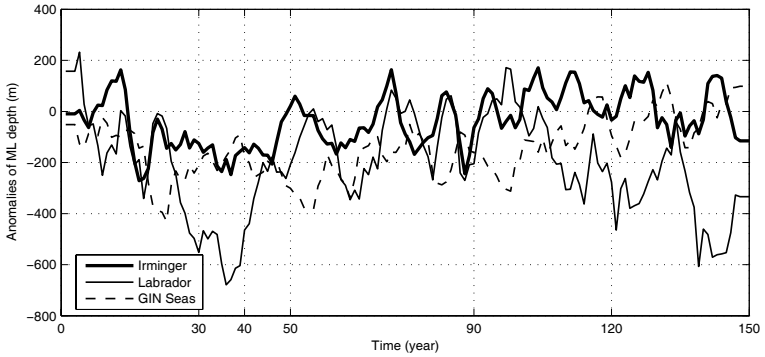

Fig. 10. The time series of the anomalies in the ML depth (FW1-CTRL) in the Labrador Sea (thin curve), the Irminger Sea (bold curve) and the GIN Seas (dashed curve).

the model drift as shown in CTRL. At the same time, the NAC also shows the recovery in strength during the last 60-yr integration in FW1 (Fig. 8). The recovered northward salt transport (Fig. 2) can counteract to the enhanced fresh water perturbation and, together with the recovered northward heat transport, can lead to the increase in SSS and SST in the NA subpolar region in FW1, which is believed as crucial mechanism for the recovery of the SPD in sub-polar regions (Fig. 6c). Otterå et al. (2004) pointed out the increased surface wind is the main reason for the recovered NAC during the last 60-yr integration in FW1. The change in the SPD will lead to change in the convective mixing, and therefore the dense water formation and the vertical stratification, which will be addressed below.

3.3 *The response of the convective mixing*

Figure 9 shows the time evolution of deep convective mixing (denoted by the area where the wintertime ML exceeds 1000 m at least once during the 150-yr integration period). First, in both CTRL and FW1, the convective mixing takes place in the Labrador Sea, the Irminger Sea and the GIN Seas in BCM. Second, it can be seen that the deep convective mixing is rather stable in the CTRL (Figs. 9a, b), whereas it is quite different in FW1 with the stronger deep mixing in the late integration period (Figs. 9c, d). Also, the extensions of convection mixing area in the Labrador Sea and the Irminger Sea are consistent with the area where the SSS and SPD are increased during the same time period in FW1.

Figure 10 shows the anomalies (FW1−CTRL) of the regional averaged ML depth in the deep convection areas. The convective mixing in the Irminger, the Labrador and the GIN Seas decreases initially in FW1 compared with CTRL and is followed by a relatively weak recovery. In the Irminger and the GIN Seas the convective mixing shows a clear and stable recovery after about year 30, while in the Labrador Sea the recovery is mainly during years 40–100.

3.4 *The response of the vertical stratification*

The calculation of the intensity of vertical stratification follows Hu (1996). In an isopycnal OGCM, within each isopycnal layer labeled by k ($k = 1, 2, \ldots$) the water mass have the same potential density, so the vertical stratification is defined by the contrast of the density along the length between two vertical adjacent layers. If using the V to denote the intensity of stratification, $k + 1$ to denote the upper layer, and $k + 2$ to denote the lower layer, and Z to denote the layer depth with downward being positive, we have:

$$V_k = \partial\rho_k/\partial Z_k = (\partial\rho_{k+2} - \partial\rho_{k+1})/(Z_{k+2} - Z_k) \quad (2)$$

For convenience, we use the difference (FW1–CTRL) in percent (Fig. 11) to show the change in the vertical density. It follows that the density stratification in the sub-polar upper ocean layers in FW1 is intensified by 15%–20% during the first 60-yr integration and such intensification disappears during the last 60-yr integration. The change is mainly in response to the changes in SSS and SPD (Figs. 4 and 5). In the sub-tropical (20°–30°N) upper ocean, the SPD is not affected as apparently as in sub-polar region (not shown); the change in the density stratification in the upper ocean is not prominent (about 0 differences).

Another feature showed by Fig. 11 is the deceasing of about 10%–20% in the deep ocean (below depth of 1500 m) stratification in both the sub-polar and sub-tropical regions during the whole FW1 integration. The more stabilized stratification in the sub-polar upper ocean suppresses the convective mixing, as a result, the production of the dense water drops down (Fig. 15). However, the responses of deep ocean vertical stratification are contrary to that in the upper ocean: an anomalous weakened stratification results from the strengthened stratification in the upper ocean. In section 3.5, we will show the impact of such

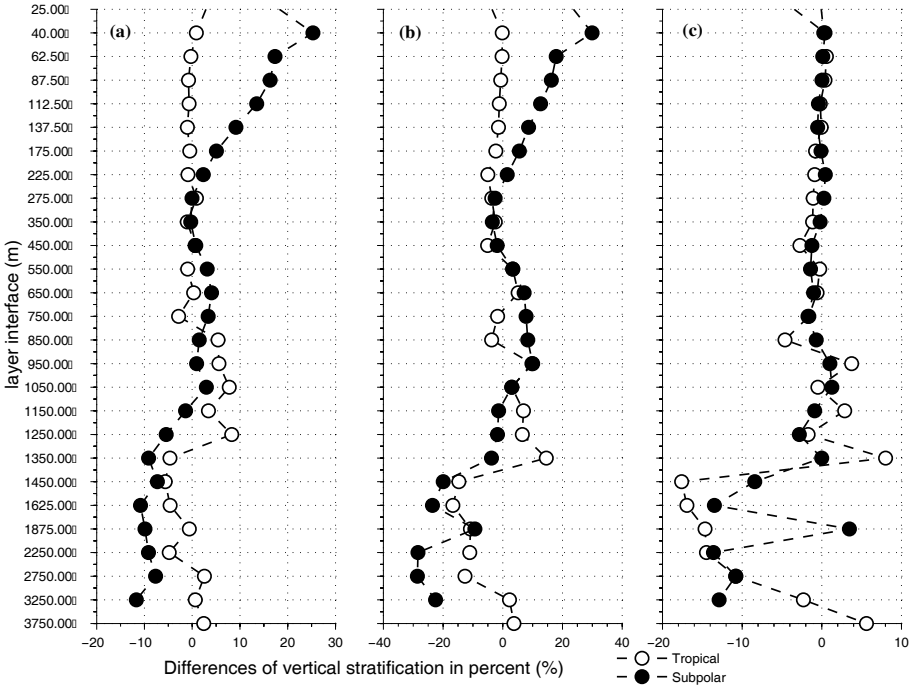

Fig. 11. The contrast (FW1-CTRL) of averaged vertical stratification profiles during the (a) first 30-yr integration , (b) the second 30-yr integration, and (c) the last 60-yr integration in the sub-polar region (45°–65°N, line with solid circles) and in the sub-tropical region (20°–30°N, line with hollow circles).

opposite responses of vertical stratification on ocean meridional circulation.

Some studies discussed that the decreasing stratification of deep ocean may cause the increasing of the upwelling (Huang, 1999; Nilsson and Walin, 2001; William et al., 2003; Wu et al., 2004), which may then intensify the pole-ward branch (Otterå et al. 2004) of the AMOC.

3.5 *The response of the upwelling in mid-low latitudes*

In MICOM, as stated earlier, the parameterization of the diapycnal mixing is stratification-dependent. Hence, the diapycnal mixing increases in the intermediate and deep ocean with the decreased vertical stratification (Fig. 11). Figure 12 shows the temporal changes of the anomalies in zonal-averaged diapycnal mixing in the Atlantic for three different integration periods. In the early integration (first 30 years), the strength of the diapycnal mixing from the intermediate to deep ocean stays almost unchanged in the low and mid-latitudes between the FW1 and the CTRL, but increases in the sub-polar intermediate to deep water (40°–60°N) in FW1 because of the reduced deep water formation. After the first 30-year integration, the strength of the diapycnal mixing increases in the Atlantic intermediate to deep water.

Additionally, there is also an increase of diapycnal mixing in the upper ocean layers in the mid- and low-latitudes in Figs. 12b and c, which is caused by a salinification (increased salinity at the mid-low latitudes in North Atlantic, figure not shown here) may be due to the previous slowdown of northward salt transport (see Fig. 2a).

The changed diapycnal mixing will influence the vertical water mass transformation, which will be diagnosed below.

Considering an idealized basin box with East-and-West-boundary-closed in which the deep dense water flows into the box through its northern lateral, and flows out of its southern lateral. The difference in volume transports between the dense inflow and the dense outflow must be transformed by the diapycnal mixing given that no deep convection takes place in the idealized basin box. Here we select sections of the Atlantic, 30°S and 24°N, to compose an approximately closed ocean region illustrated in Fig. 13. Here we calculate the difference in southward-flowing dense water transports (water mass with potential densities greater than 27.63) across the zonal sections of 30°S and 24°N as an indication to the vertical mass transformation within the low latitudes in NA.

Figure 14 shows the time series of the vertical water mass transformation in the FW1 and the CTRL with their second-order polynomial least-square fit to

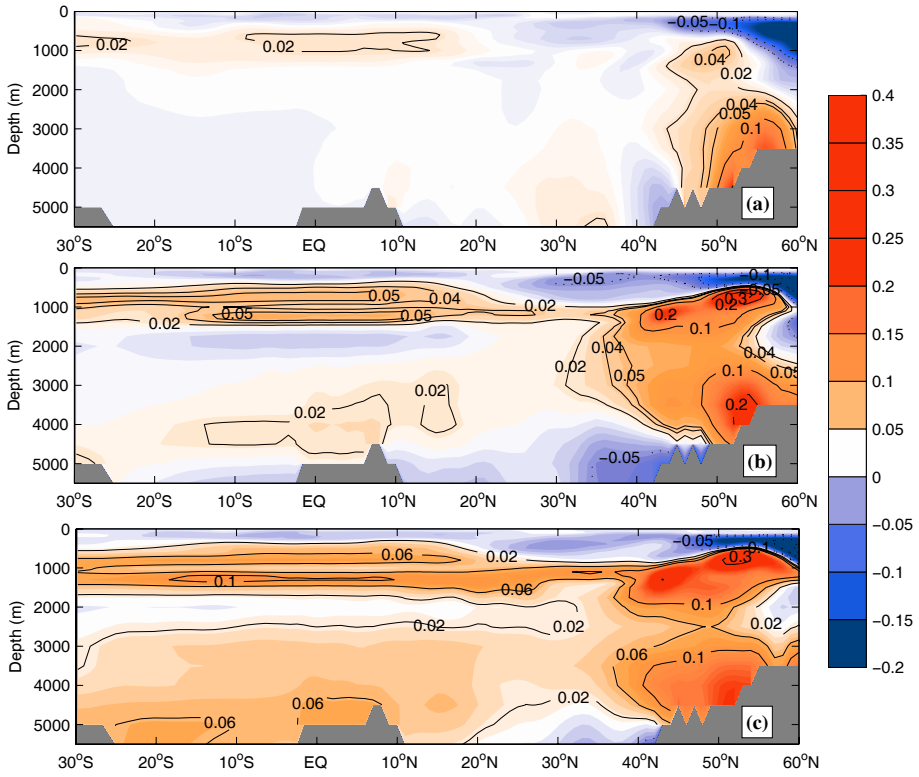

Fig. 12. The temporal evolution of the anomalies (FW1−CTRL) in zonal-averaged $\mathrm{m}^{-2}\ \mathrm{s}^{-1}$) for (a) the first 30-yr, (b) the ns.

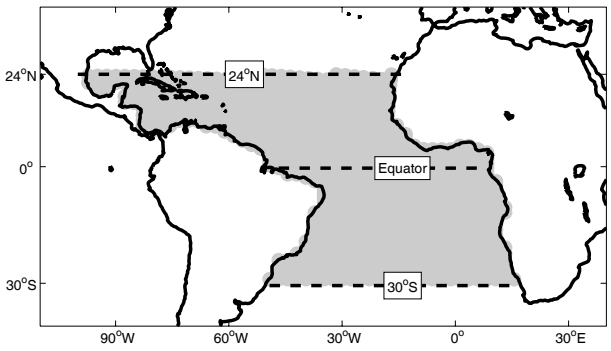

Fig. 13. The selected region for diagnosing the vertical water mass transformation in the Atlantic.

the 150-yr integration. In CTRL, the vertical mass transformation in the low-latitudes (30°S–24°N) of the Atlantic Ocean exhibits a weak and steady trend with a mean value about 2.6 Sv, while in FW1, it shows an apparent increasing trend in FW1. The water transformation with a mean value of 4.3 Sv during the last 100-yr integration in FW1 is much higher than that in CTRL with a mean value of 2.7 Sv during the last 100-yr integration. Gao et al. (2003) found that the basin-scale increase in diapycnal mixing by about 5%–10% can lead to increased upwelling by 1 Sv, and Otterå et al. (2004) speculated that such an increase in upwelling may be one of the reason for the recovery of AMOC in FW1. Our results show that the water mass transformation in the tropical Atlantic does increase due to the increase in diapycnal mixing in FW1.

3.6 *The response of the rate of deep water formation*

Figure 15 shows the temporal changes of the dense water formation rate in FW1, which is defined as the southward dense water transport (water mass with potential densities equals to or greater than 27.63) across the southern boundaries of the deep convection area (Fig. 9). The dense water formation in the Labrador, the Irminger and the GIN Seas in FW1 decreases during the first 30-yr integration and gradually recovers in the later integration. The time series of the dense water formation is consistent with the AMOC (Fig. 1). During the first 30-yr integration, the enhanced freshwater input to the high northern latitudes causes the more stabilized vertical stratification, leading to the weakened convective mixing, which in turn reduces the dense water formation in the sub-polar region and the GIN Seas.

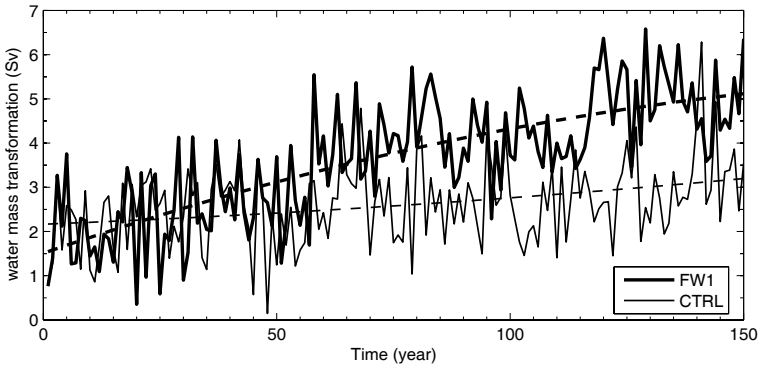

Fig. 14. The time changes of the vertical water mass transformation in the low-latitudes (30°S–24°N) of the Atlantic in CTRL and FW1. Additionally, their second-order polynomial least-square fits to the 150-yr integration are denoted by the dashed lines.

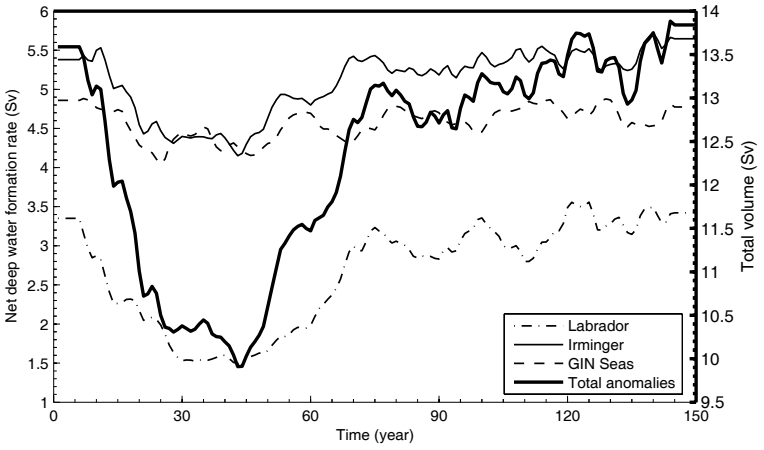

Fig. 15. The temporal changes of the dense water formation rate in the Labrador Sea (dot-dashed curve), the Irminger Sea (thin curve), the GIN Seas (dashed curve) and the total of them (bold curve) in FW1. The total volume is scaled by the right y-axis.

4. Discussion

A number of studies suggest that a large freshwater input to the northern high-latitude ocean might create a stable stratification, and thereby shut down the deep water formation (Tziperman, 2000, Zhou et al., 2005). But also, as reported by Furevik et al. (2003), the poleward transport of the salt is crucial for the formation of the dense water in the Labrador and the GIN Seas (Furevik et al., 2003; Otterå et al., 2004): If the SSS in convective mixing regions recovers, the deep water formation may restart.

In the North Atlantic sub-polar region, density variations are mainly determined by the salinity variations (Furevik et al., 2003; Otterå et al., 2004). In the BCM, The artificially added freshwater input leads to the rapid decreasing of the SSS over the sub-polar regions (Fig. 4a). Consequently, the sea surface water is less dense (Fig. 4c and Fig. 5b), leading to a more stabilized vertical stratification in the upper ocean of the northern high latitudes (Fig. 11) and thereafter reduce the strength of the winter time convective mixing (Fig. 9 and Fig. 10). This final results in the less dense water formation (Fig. 15) and the weakened AMOC (Fig. 1) during the early phase of the enhanced freshwater input. It also should be noted that the southward overflow across the GSR deceased rapidly (Fig. 3) during the early phase of the enhanced freshwater input. These results in the high latitudes are consistent with a large body of numerical ocean studies (e.g., Marotzke and Scott, 1999; Park and Bryan, 2000).

The bulk of the dense water formation feeding the North Atlantic Ocean via the GSR is formed within the Nordia Seas (Isachsen et al., 2007). In some ocean models using constant vertical mixing, if the deep water formation is stopped by the freshening in the high

latitudes, the AMOC will be shut down or weakened without recovery (Manabe and Stouffer, 1995; Schiller et al., 1997). Consequently, the northward salt transport carried by the NAC is reduced and the SSS in the high northern latitudes cannot be recovered until the enhanced freshwater forcing is removed. However, some recent studies (Huang, 1999; Nilsson and Walin, 2001; William et al., 2003; Wu et al., 2004) suggest that the strength of AMOC might be dominated by the small-scale diapycnal mixing process. That is, with the decreasing of the deep water formation and the southward intermediate and deep overflow across GSR into the NA, the vertical density stratification in the Atlantic weakens with time. Such responses can trigger the broad upward diapycnal flow in the low and mid latitudes, and furthermore, they suggest that the outcome is a stronger northward ocean transport and finally a stronger AMOC.

In ocean models whose basin-scale vertical mixing coefficient is constant or only depth-dependent, such as the Stommel's classical model (Stommel, 1961) and some other ocean models (e.g., Bryan, 1987; Zhang et al., 1999; Park and Bryan, 2000), the simulated AMOC can not recover with the continuously added freshwater perturbation in the high northern latitudes. On the other hand, if the stratification-dependent diapycnal mixing is applied to the models, the vertical mass transformation will be regulated by the vertical stratification within the intermediate to deep ocean in the low latitudes (Huang, 1999).

In MICOM, the diapycnal mixing is parameterized as stratification dependent. It is found that the overflow waters (OW) from the GIN Seas into NA, the penetration of the western boundary currents, the ventilation of the subtropical surface waters, the vertical density stratification and the meridional overturning are all critically dependent on the applied isopycnal and diapycnal mixing (Gao et al., 2003). As to our results, the SSS, the SPD and the rate of the NADW formation drops down because of the stabilization of the upper ocean vertical stratification during the first 50-yr integration in the freshwater perturbation experiment. However, because the stabilized vertical stratification in the upper ocean of high northern latitudes prevents the formation of dense water, the deep dense water flowing into the mid-low latitudes of NA will decrease. Consequently, vertical stratification weakens in the deep ocean over the entire low and mid latitudes (Fig. 11), and then the diapycnal mixing within the NA increases (Fig. 12). With the increased diapycnal mixing, the vertical mass transformation at low and mid latitudes within NA is intensified (Fig. 15). Consequently, the northward branch of AMOC and its transport of the volume, heat and salt into high latitudes is recovered (Fig. 2). Sufficient saline waters from the West Tropical North Atlantic (WTNA) region may counteract the artificially released freshwater in the BCM (Otterå et al. 2004). Finally, such a response results in the recovered SSS and SPD (Fig. 5) in the high latitudes, leading to the recovery of the NADW formation (section 3.5). Similar results are obtained by Vellinga et al. (2002): The gradually increased salinity re-triggers the deep water formation in the Greenland and Norwegian Seas and the Labrador Sea, leading to the recovery of the AMOC.

5. Conclusion

The transient response of the simulated AMOC in the BCM under the freshwater perturbation is revisited. It shows that the vertical mixing/diapycnal mixing parameterized as stratification dependent plays an import role in the transient response of the simulated AMOC by regulating the strength of the upwelling at the mid-low latitudes in NA. The transient response of the AMOC under the continuously and constantly added fresh water input over 150 years shows an initial slow-down during the first 50 years followed by a gradual recovery. First, the upper ocean freshening in the high latitudes causes the reduction in the sea surface density leading to stabilized vertical stratification in the GIN Seas and NA sub-polar region, and, therefore, resulting in weakened NADW formation. Second, the reduced southward-flowing dense water will weaken the deep ocean stratification in the mid-low latitudes of NA and intensify the diapycnal mixing which is parameterized as stratification dependent. The increased diapycnal mixing will bring about more vertical mass transformation and contribute to the recovery of the northward transport of volume, heat and salt into the GIN Seas and the NA sub-polar region. This will recover the dense water formation there by reducing the upper ocean stratification with restored SSS.

Acknowledgements. This work was supported by the 100-Talent Program of CAS granted to Prof. Gao Yongqi and CAS Project "IAP OGCM Improvement and Coupling to AGCM and Ocean Carbon Cycle" (Grant No. KZCX2-YW-218). The authors are also grateful to Dr. Odd Helge Otterå for providing the model outputs.

REFERENCES

Aagaard, K., and E. C. Carmack, 1989: The role of the sea ice and other freshwater in the Arctic circulation. *J. Geophys. Res.*, **94**, 14485–14498.

Bentsen, M., H. Drange, T. Furevik, and T. Zhou, 2004: Simulated variability of the Atlantic meridional over-

turning circulation. *Climate Dyn.*, **22**, 701–720.

Bleck, R., C. Rooth, D. Hu, and L. T. Smith, 1992: Salinity-driven thermocline transient in a wind- and thermohaline-forced isopycnic coordinate model of the North Atlantic. *J. Phys. Oceanogr.*, **22**, 1485–1505.

Bryan, F., 1987: Parameter sensitivity of the primitive equation ocean general circulation models. *J. Phys. Oceanogr.*, **17**, 970–985.

Déqué, M., C. Dreveton, A. Braun, and D. Cariolie, 1994: The ARPEGE/IFS atmosphere model: A contribution to the french community climate modelling. *Climate Dyn.*, **10**, 249–266.

Dickson, R. R., T. J. Osborn, J. W. Hurrell, J. Meincke, W. Turrell, S. Dye, and J. Holfort, 2002: Rapid freshening of the deep North Atlantic Ocean over the past four decades. *Nature*, **416**, 832–837.

Furevik, T., M. Bentsen, and H. Drange, 2003: Desciption and evaluation of the Bergen Climate Model: ARPEGE coupled with MICOM. *Climate Dyn.*, **21**, 27–51.

Gao, Y. Q., H. Drange, and M. Bentsen, 2003: Effects of the diapycnal and isopycnal mixing on the ventilation of the CFCs in the North Atlantic in an isopycnal coordinate OGCM. *Tellus*, **55B**, 837–854.

Garabato, A., K. L. Polzin, B. A. King, K. J. Heywood, and M. Vicbeck, 2004: Widespread intense turblent mixing in the Southern Ocean. *Science*, **303**, 210–213.

Gargett, A., 1984: Vertical eddy in the ocean interior. *J. Mari. Res.*, **42**, 359–393.

Garrett, C., and L. St. Laurent, 2002: Aspects of deep ocean mixing. *J. Phys. Oceanogr.*, **58**, 11–24..

Hu, D., 1996: The computation of diapycnal diffuse and advective scalar fluxes in multilayer Isopycnal-Coordinate ocean models. *Mon. Rev. Wea.*, **124**, 1834–1851.

Huang, R. X., 1999: Mixing and energetic of the oceanic thermohaline circulation. *J. Phys. Oceannogr.*, **29**, 727–746.

Isachsen, P. E., C. Mauritzen, and H. Svendsen, 2007: Dense Water formation in the GIN Seas diagnose from sea surface buoyancy fluxes. *Deep-Sea Res. I*, **54**, 22–41.

Manabe, S., and R. J. Stouffer, 1994: Multiple-century response of a coupled ocean-atmosphere model to an increase of atmosphere carbon Dioxide. *J. Climate*, **7**, 5–23.

Manabe, S., and R. J. Stouffer, 1995: Simulation of abrupt climate change induced by freshwater input to the North Atlantic Ocean. *Nature*, **378**, 165–167.

Manabe, S., and R. J. Stouffer, 1997: Coupled ocean-atmosphere model response to freshwater input: Comparison to Younger Dryas event. *Paleoceanography*, **12**, 321–336.

Marotzke, J., and J. R. Scott, 1999: Convective mixing and the thermohaline circulation. *J. Phys. Oceanogr.*, **29**, 2962–2970.

McDougall, T., and W. K. Dewar, 1998: Vertical mixing and cabbeling in layered models. *J. Phys. Oceanogr.*, **28**, 1458–1480.

Mohanmmad, R., and J. Nilsson, 2004: The role of diapycnal mixing for the equilibrium response of the thermohaline circulation. *Ocean Dynamics*, **54**, 54–65.

Moum, J., D. Caldwell, J. Nash, and G. Gunderson, 2002: Observations of boundary mixing over the continental slope. *J. Phys. Oceanogr.*, **32**, 2113–2130.

Munk, W. H., and C. Wunsch, 1998: Abyssal recipes 2: energetic of tidal and wind mixing. *Deep-Sea Res. I*, **45**, 1977–2010.

Nilsson, J., and G. Walin, 2001: Freshwater forcing as a booster of thermohaline circulation. *Tellus*, **53A**, 629–641.

Oliver, K. I. C., A. J. Watson, and D. P. Stevens, 2005: Can limited ocean mixing buffer repid climate change? *Tellus*, **57A**, 676–690.

Otterå, O. H., H. Drange, M. Bentsen, N., G, Kvamstø, and D. B. Jiang, 2004: Transient response of the Atlantic meridional overturning circulation to enhanced freshwater input to the Nordic Seas-Arctic Ocean in the Bergen Climate Model. *Tellus*, **56A**, 342–361.

Park, Y. G., and K. Bryan, 2000: Comparison of thermally driven circulation from a depth-coordinate model and an isopycnal model. Part I: Scaling-law sensitivity to vertical diffusivity. *J. Phys. Oceanogr.*, **30**, 590–605.

Peterson, B. J., R. M. Holmes, J. W. McClelland, C. J. Vorosmarty, R. B. Lammers, A. I. Shiklomanov, I. A. Shiklomanov, and S. Rahmstorf, 2002: Increasing river discharge to the Arctic Ocean. *Science*, **298**, 2171–2173.

Rahmstorf, S., 1996: On the freshwater forcing and transport of the Atlantic thermohaline circulation. *Climate Dyn.*, **12**, 799–811.

Rahmstorf, S., and A. Ganopolski, 1999: Long-term global warming scenarios computed with an efficient coupled climate model. *Climatic Change*, **43**, 353–367.

Schiller, A., U. Mikolajewicz, and R. Voss, 1997: The stability of the thermohaline circulation in a coupled ocean-atmosphere general circulation model. *Climate Dyn.*, **13**, 325–347.

Simonsen, K., 1996: Heat budgets and freshwater forcing of the GIN Seas and the Arctic Ocean. Ph. D. dissertation, Nansen Environmental and Remote Sensing Center, Bergen, Norway, 132pp. (in Norwegian).

Stommel, H. and A. B. Araons, 1960: On the abyssal circulation of the world ocean: I. Stationary flow patterns on a sphere. *Deep-Sea Res. I*, **6**, 140–154.

Stommel, H., 1961: Thermohaline covection with two stable regimes of flow. *Tellus*, **13A**, 224–230.

Tziperman, E., 2000: Proximity of the present day thermohaline circulation to an instability threshold. *J. Phys. Oceanogr.*, **30**, 90–104.

Vellinga, M., R. A. Wood, and J. M. Gregory, 2002: Processes governing the recovery of a perturbed Thermohaline Circulation in HadCM3. *J. Climate*, **15**,

764–780.

William, R. B., J. R. Scott, and K. A. Emanuel, 2003: Transient Diapycnal Mixing and the Meridional Overturning Circulation. *J. Phys. Oceanogr.*, **34**, 334–341.

Wu, Peili, R. Wood, and P. Stott, 2004: Does the recent freshening trend in the North Atlantic indicate a weakening thermohaline circulation? *Geophys. Res. Lett.*, **31**, L02301, doi: 02310.01029/02003GL018584.

Wunsch, C., and R. Ferrari, 2004: Vertical mixing, energy and the general circulation of the oceans. *Annual reviews of Fluid Mechanics*, **36**, 281–314.

Zhang, J., R. W. Schmitt, and R. X. Huang, 1999: The relative influence of diapycnal mixing and hydrological forcing on the stability of thermohaline circulation. *J. Phys. Oceanogr.*, **29**, 1096–1108.

Zhang, X., M. Ikeda, and J. E. Walsh, 2004: Arctic sea-ice and freshwater changes driven by the atmospheric leading mode in a coupled sea ice-ocean model. *J. Climate*, **16**, 2159–2177.

Zhou, T. J., R. C. Yu, X. Y. Liu, Y. F. Guo, Y. Q. Yu, and X. H. Zhang, 2005: Weak response of the Atlantic thermohaline circulation to an increase of atmosphere carbon dioxide in IAP/LASG Climate System Model. *Chinese Science Bulletin*, **50**, 592–598.